Role of Guanidyl Moiety in the Insertion of Arginine and N_α-Benzoyl-L-argininate Ethyl Ester Chloride in Lipid Membranes

A. C. Fonseca,[‡] M. A. Frías,[†] A. M. Bouchet,[†] S. Jarmelo,[‡,§] P. N. Simões,[‡] R. Fausto,[§] M. H. Gil,[‡] F. Lairion,[†] and E. A. Disalvo*,[†]

Laboratory of Physical Chemistry of Lipid Membranes, Department of Analytical Chemistry and Physical Chemistry, Pharmacy and Biochemistry, University of Buenos Aires Junín 956 2° piso (1113), Buenos Aires, Argentina, Department of Chemical Engineering, University of Coimbra, Polo II, Pinhal de Marrocos, 3030-790 Coimbra, Portugal, and Department of Chemistry, University of Coimbra, 3004-535 Coimbra, Portugal

Received: February 2, 2010; Revised Manuscript Received: March 26, 2010

Guanidyl moieties of both arginine (Arg) and N_α-benzoyl-L-argininate ethyl ester chloride (BAEE) are protonated in all environments studied, i.e., dry solid state, D_2O solutions, and dry and hydrated lipids as suggested by DFT(B3LYP)/6-31+G(d,p) calculations. Arg and BAEE are able to insert in the lipid interphase of both DMPC and DOPC monolayers as revealed by the observed decrease in the membrane dipole potential they induce. The larger decrease in the dipole potential induced by BAEE, compared to Arg, can be explained partially by the higher affinity of the hydrophobic benzoyl and ethyl groups for the membrane phase, which allows an easier insertion of this molecule. FTIR studies indicate that the guanidyl moiety of Arg is with all probability facing the hydrophobic part of the lipids, whereas in BAEE this group is facing the water phase. Zeta potential measurements provide a direct evidence that Arg orients in the lipid interphase of phosphatidylcholine (PC) bilayers with the negative charged carboxylate group ($-COO-$) toward the aqueous phase.

Introduction

The interaction of proteins with different types of membranes has been explained in terms of the insertion of some amino acids at different depths of the bilayer.[1−4] Some models postulate the role of individual amino acids that can partition into the bilayer. The free energy of partitioning of an amino acid side chain from water into the cell membrane is one of the critical parameters for understanding and predicting membrane peptide stability and understanding membrane protein function. Transmembrane segments are generally very hydrophobic but may contain hydrophilic residues which are important for the structure or function of the protein.[5] Polycationic peptide insertion is mainly due to electrostatic interactions and specific interactions with phosphatidycholine (PC) head groups.[6,7]

Among positively charged amino acids, L-arginine (Arg) is an important component of several peptides and proteins.[8,9] The Arg side chain is constituted by a polar guanidyl moiety located at the end of a four-atoms hydrophobic carbon chain, then bearing simultaneously polar and apolar regions. In recent years, there has been great interest concerning the protonation state of Arg residues in a lipid bilayer environment.[10,11]

MacCallum et al.[12] reported an insight on the preferred location and orientation of the Arg side chain, as well as its preferred charge states in lipid bilayers, by means of molecular dynamic studies. It has been shown that Arg may be either charged or uncharged at the center of the membrane[5,12] and that the mechanism of penetration of Arg in a membrane might be related with the formation of water defects connecting its side chains to bulk water.[12] These water defects would dominate the energetics of partitioning and participate in a process in which water molecules in the hydrophobic phase of the membrane should also be involved.[12−14] Thus, unlike other ionizable amino acids, such as lysine, glutamic, and aspartic acids, which become uncharged well before reaching the center of the membrane, charged Arg molecules can exist at the center of the membrane by the rapid formation of water defects.[13]

The main goal of this paper is the elucidation of both the preferred location and charge state of the guanidyl moiety of Arg in the membrane. Accordingly, the insertion of Arg monomers in PC bilayers was compared with that of the Arg derivative, N_α-benzoyl-L-argininate ethyl ester chloride (BAEE), in which the negative carboxylate moiety ($-COO^-$) of Arg is replaced by the neutral hydrophobic carboxylic ethyl ester group $[-C(=O)OC_2H_5]$, and one of the hydrogen atoms of the α-amino group ($-NH_2$) is replaced by the hydrophobic and voluminous benzoyl moiety ($-C(=O)C_6H_6$), thus forcing the guanidyl group to stabilize at the water−membrane interphase.

The effect of the insertion of Arg and BAEE in membranes was then investigated at a macroscopic scale by measuring the zeta potential of bilayers and dipole potential of monolayers of PC and, at a molecular level, by means of FTIR spectroscopy in dry and hydrated films of the amino acids interacting with lipids. In addition, structural, energetic, spectroscopic, and physical (dipole moments) properties of both Arg (in its canonic and zwitterionic forms) and of its BAEE derivative (canonic and cationic forms) were studied theoretically at the DFT(B3LYP)/6-31+G(d,p) level.

* Corresponding author. Phone: 54 11 39648249. Fax: 54 11 45083645. E-mail: eadisal@yahoo.com.ar.
† Department of Analytical Chemistry and Physical Chemistry, Pharmacy and Biochemistry, University of Buenos Aires Junín 956 2° piso (1113).
‡ Department of Chemical Engineering, University of Coimbra.
§ Department of Chemistry, University of Coimbra.

Insertion of Arg and BAEE in Lipid Membranes

J. Phys. Chem. B, Vol. 114, No. 17, 2010 **5947**

TABLE 1: DFT (B3LYP)/6-31+G(d,p) Zero-Point Corrected Total (E_0) and Relative (ΔE_0) Energies and Dipole Moments (μ) for Canonic and Ionic Relevant Forms of Arg and BAEE in Vacuum and Water Solution

molecule	form	E_0/hartree		ΔE_0/(kJ mol^{-1})		μ/Debye	
		vacuum	water	vacuum	water	vacuum	water
Arg	canonic	−606.3778	−606.4297	0	0	8.43	12.59
	zwitterion I	[a]	−606.4080	[a]	56.9	[a]	20.07
	zwitterion II	−606.3712	−606.3937	17.2	94.5	6.40	14.09
BAEE	canonic	−1029.2752	−1029.2964	1080.4	1206.9	5.16	7.25
	cation	−1029.6867	−1029.7561	0	0	10.35	13.53

[a] During the gas-phase optimization, the zwitterionic form of Arg converged to the canonical one.

Materials and Methods

Chemicals. Dimyristoyl phosphatidylcholine (DMPC) and dioleoyl phosphatidylcholine (DOPC) were obtained from Avanti Polar Lipids, Inc. (Alabaster, AL) and used as received. The purity of lipids was checked by thin layer chromatography using a chloroform:methanol:water mixture as running solvent. Arg and BAEE were obtained from Sigma-Aldrich (Saint Louis, MO). Chloroform and KCl were analytical grade. Water was Milli-Q quality.

Dipole Potential Measurements. Dipole potentials (Ψ_D) were determined in lipid monolayers formed at the air−water interphase at saturation. Aliquots of chloroform solutions of the two lipids tested were spread on a clean water surface or aqueous solutions with Arg or BAEE at different concentrations and left to reach constant pressures, until no changes were observed with further additions of the lipids. At this saturation condition, lipids in the monolayer are in equilibrium with lipids in the subphase.[15−17]

Under these conditions, the values of interfacial potential (V_{surf}) were determined through a high impedance circuit, by means of an Am ionizing electrode (α-emissor) placed on the monolayer and a reference electrode immersed in the aqueous subphase (KCl 1 mM) using the following expression: $V_{surf} = V_{Ag/AgCl} − V_{grd} = V_{solution} − V_{grd}$, where $V_{Ag/AgCl}$ is the potential of the reference electrode and V_{grd} is the potential of the shield covering the ionizing electrode.

Temperature was set at the values indicated in each assay (mostly, 18 and 28 °C) and measured with a calibrated thermocouple immersed in the subphase and maintained within ±0.5 °C.

The Ψ_D of the monolayer was evaluated as $\Psi_D = V_{surf} − V_{lip}$, where V_{surf} is the potential of the clean surface (without lipids) and V_{lip} is the potential after the monolayer formation. Ψ_D is related with the area (A) according to $\Psi_D = \mu_\perp/A\varepsilon_o\varepsilon$, where $\mu_\perp$ is the average component of the lipid molecular dipole moment including membrane-associated water molecules perpendicular to the plane of the membrane; ε_o is the permittivity of free space; and ε is the local dielectric constant.[18]

Zeta Potential Measurements. Zeta potentials were determined by measuring the electrophoretic mobility of multilamellar liposomes (MLVs) in a Zeta-Meter System 3.0 equipment, at 18 ± 2 °C. The voltage was fixed at 75 V.

MLVs were prepared by dispersing the dry lipid films in Arg or BAEE solutions with KCl 1 mM, above the transition temperatures of the lipids (T_m DMPC = 24 °C; T_m DOPC = −5 °C), for 60 min. In another series of experiments, liposomes were prepared by dispersing the lipids in a KCl aqueous solution, and different concentrations of Arg or BAEE (5−20 mM) were added to the liposome dispersion and incubated for 1 h above the phase transition temperature of both lipids (ca. 35 °C). Then, the liposome samples were cooled to 18 °C and transferred to the measuring cell. Measures were done at 18 °C for a total lipid concentration of 52 μM.

A total of 20 measurements were carried for each liposome batch. Data reported are the average of the measurements done for each condition with at least three different batches of liposomes. The pH of the solution of Arg and BAEE liposomes were controlled before and after the zeta potential measurements. No important variations were found.

FTIR Measurements. Spectra of the solid state samples were obtained for the compounds dispersed in KBr pellets, at a relative humidity (RH) of 33−35%.

For spectra determination in solutions, lipids were dispersed in Arg and BAEE D$_2$O solutions.

The water content of the dry lipid films was estimated as RH by means of the spectral parameter defined as the ratio of the integral absorbance of the $\nu_{1,3}$OH band of water, centered near 3400 cm^{-1}, and that of the C−H stretching region (3000−2750 cm^{-1}), after baseline correction, in consonance with Pohle et al.[19] For fully hydrated lipid samples, 3−5 mg of the dried sample was mixed with 30−50 μL of D$_2$O by vigorously vortexing at temperatures above the transition temperature of the lipids (see above). The dispersion was then squeezed between two AgCl windows, used as an optical substrate.

A FTIR Nicolet TM 380 spectrophotometer, provided with a DTGS detector and a KBr beamsplitter, was used. A total of 64 scans were co-added for solid samples and of 320 scans for hydrated samples, in both cases with 2 cm^{-1} resolution. A number of different samples (no less than three) were processed to obtain a standard deviation below the resolution of the equipment. Whenever necessary, Fourier self-deconvolution was applied to estimate the frequencies of the component bands (band narrowing factors: 1.6−2.2), followed by curve fitting to obtain band widths and intensities.

Calculations. The theoretical calculations were based on density functional theory (DFT)[20,21] and performed with the Gaussian 03 package,[22] using the Becke-style three-parameter with the Lee−Yang−Parr correlation functional (B3LYP)[23−25] and the 6-31+G (d,p) Pople-type basis set.[26,27] The simulations were carried out both in vacuum and taking into account solvent (water) effects by using the polarized continuum model, PCM,[28−33] at the same level of theory.

Results and Discussion

To determine the protonated states of Arg and BAEE in the investigated environments (dry solid state, D$_2$O solution, and in interaction with dry and hydrated lipids), B3LYP/6-31+G(d,p) calculations were performed on canonic and ionic forms of these two species. Besides minimum energy structures, energies, and IR spectra, the total dipole moments for each species were obtained (Table 1; Figure 1). For Arg, zwitterionic forms where the protonated groups are the guanidyl (zwitterion I) and the α-amino group (zwitterion II) were considered. The calculations in vacuum predicted both zwitterionic forms to converge to different canonic forms (see Figure 1). While zwitterion I has converged to the most stable canonic form, the
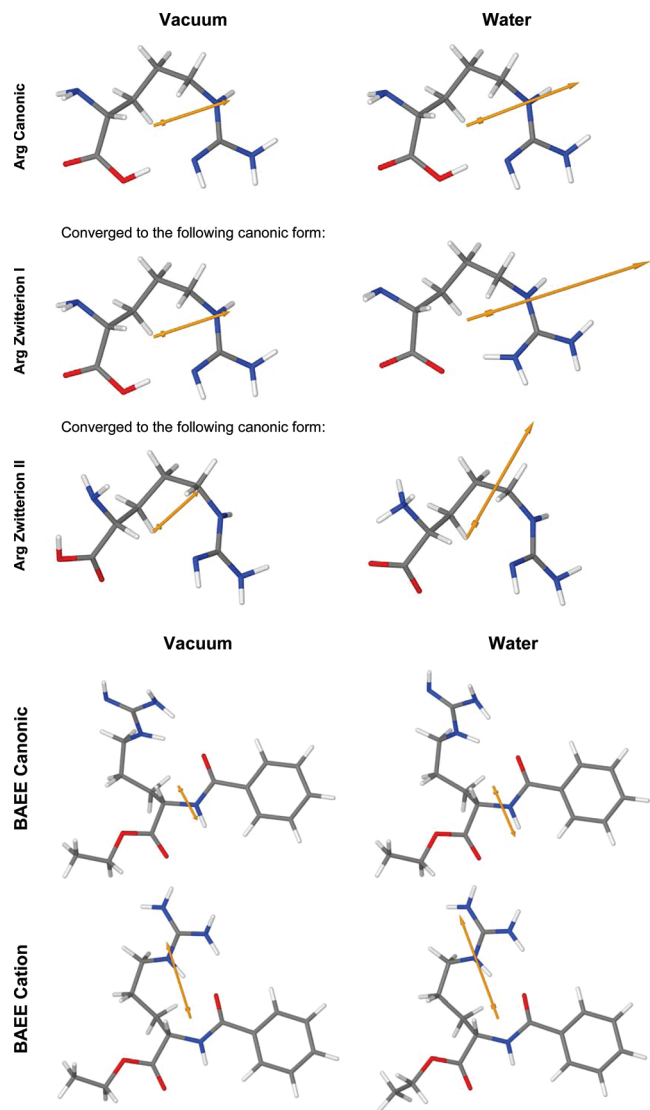
Figure 1. Schematic drawings of Arg and BAEE in the charge states studied, showing the orientation of the total dipole moments.

Figure 2. Effect of Arg and BAEE on the zeta potential (ζ) of DMPC and DOPC liposome, at 18 °C. DMPC ($\square$)/DOPC ($\triangle$) Liposomes prepared by dispersing a dry film in Arg or BAEE solutions of the indicated concentrations, at a temperature above the phase transition. DMPC ($\blacksquare$)/DOPC ($\blacktriangle$) Liposomes prepared in water and incubated at ca. 35 °C in solutions of Arg or BAEE of the indicated concentrations. Lines are only added to visualize the trend.

optimization of zwitterion II has led to a canonic conformer energetically less favorable by ca. 17 kJ mol^{-1} (see Table 1). On the other hand, the calculations in water (PCM method) predicted the guanidinium zwitterionic form (I) to be considerably more stable than the α-ammonium form (II) [E(II−I) = 37.7 kJ mol^{-1}; see Table 1]. This is in accordance with the well-known higher basicity of the guanidyl moiety (the pK_a values of the polyfunctional Arg amino acid are 2.1, 9.0, and 12.5 for the acid, amino, and guanidyl moieties, respectively).[34] In the case of BAEE, the two forms investigated are analogous of those considered for Arg, i.e., the canonical form and the cationic species with the charge located in the guanidyl moiety. The importance of the guanidyl protonated species for the present study was not just stressed by our own calculations but also by the quite recent work of Im et al.,[35] which reports that the zwitterionic form of Arg with a protonated guanidyl moiety (I) is more stable than the canonical form even when solvated by just a few water molecules. One can then confidently state that in all environments investigated in the present study in both Arg and BAEE the guanidyl group is protonated.

The zeta potentials of DMPC and DOPC liposomes prepared in water, at 18 °C, show a shift to negative values when titrated in the presence of increasing concentrations of Arg after their incubation above th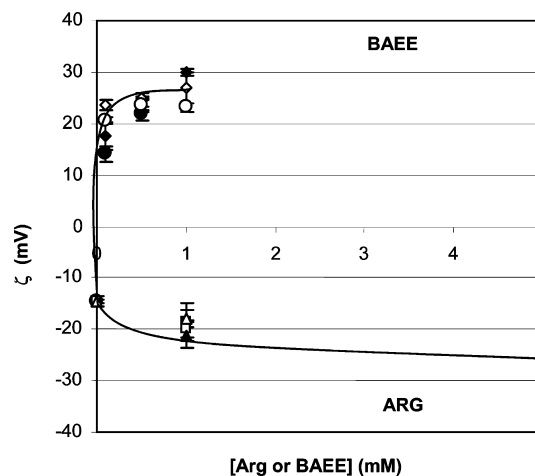e phase transition temperature. Identical results were obtained when the liposomes were prepared in Arg solutions of similar concentrations and measured at the same temperature (see Materials and Methods), as shown in Figure 2.

The pH of the systems was controlled before and after the measurements. No buffer was added to avoid interferences in the surface charge adsorption measures. In this condition, it is interesting to note that the same shift was observed in liposomes in the fluid state and with those in the gel state after their incubation above the phase transition temperature. Moreover, it is important to notice that even for the two unbuffered solutions, Arg and BAEE, they caused qualitative opposite shifts of the zeta potential.

In Figure 2, one can observe that the same protocol, using BAEE, produces a zeta potential shift to positive values. In addition, it should also be stressed that, in this latter case, the change in the zeta potential is observed at much lower concentrations. The shift to negative zeta potential, observed when Arg is inserted in membranes, suggests that Arg is facing the carboxylate group to the water phase. In turn, this allows concluding that the Arg guanidyl moiety should be oriented toward the membrane hydrophobic core. On the other hand, in the case of BAEE, it is not difficult to determine the position of the guadinyl moiety because the shift of zeta potential to net positive charge indicates that it is facing the water phase.

The fact that both Arg and BAEE are able to insert in the lipid interphase of both DMPC and DOPC monolayers is clearly revealed by the observed decrease in the membrane dipole potential they induce (Figure 3). However, BAEE promotes a much larger decrease than Arg for similar concentrations. For example, when the compounds are inserted in the lipid interphase of DMPC at a 20 mM substrate concentration, the induced decrease in the dipole potential is ca. 300 mV for BAEE and only ca. 50 mV for Arg. Even at concentrations as high as 100 mM the decrease induced by Arg (ca. 110 mV; data not shown) is smaller than that produced by a 20 mM BAEE concentration. In summary, the decrease in the dipole potential induced by BAEE in condensed monolayers of DMPC is ca. 6-fold higher than that obtained for a similar concentration of Arg. On the
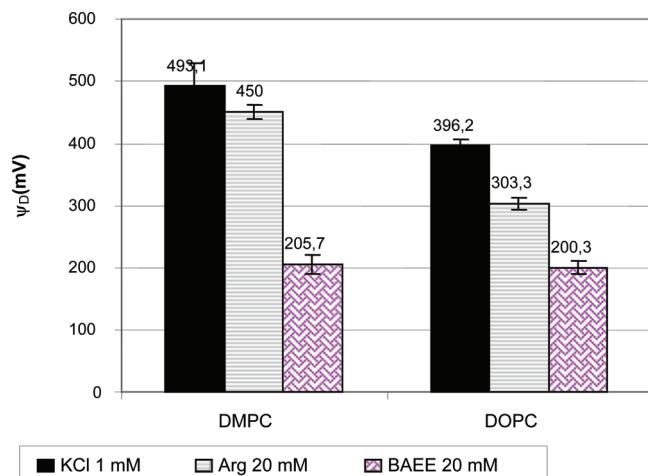
Insertion of Arg and BAEE in Lipid Membranes

J. Phys. Chem. B, Vol. 114, No. 17, 2010 **5949**

Figure 3. Effect of Arg and BAEE (20 mM) on the dipole potential of DMPC and DOPC monolayers.

other hand, the effect of BAEE insertion in DOPC monolayers was found to be only 2-fold larger with respect to Arg (see Figure 3).

The larger decrease in the dipole potential induced by BAEE, compared to Arg, can be explained partially by the higher affinity of the hydrophobic benzoyl and ethyl groups for the membrane phase, which allows an easier insertion of these species. In addition, the picture derived from zeta potentials indicates that the guanidyl moiety of BAEE is exposed to the water phase. Therefore, the dipole moment of BAEE opposes the base dipole potential of the lipid (which is positive inside the membrane), thus explaining the drastic decrease in the dipole potential it induces for both DMPC and DOPC compared to that resulting from the interaction of the lipids with Arg.

On the other hand, in the case of Arg, the positively charged guanidyl moiety seems to be located in the membrane, with all probability at the interphase, counteracting both the phosphate and carbonyl dipoles of the lipids. Indeed, if the orientation of the guanidyl moiety was toward the hydrocarbon core of the lipids, there would be two crucial points which would be difficult to understand. First, how could the positive charge of that moiety to be stabilized in the positively charged region of the lipid? Second, if this was true, then the dipole moment of Arg would be oriented in the same direction as the base dipole moment of the membrane, and thus the dipole potential should increase, which is inconsistent with the observations (see Figure 3).

The smaller reduction in the dipole potential of the membranes caused by the insertion of Arg (compared to that due to BAEE insertion) and the simultaneous negative zeta potential of the Arg-interacting membrane seem in fact to be easily explained as follows: the insertion of the guanidyl group at the interphase, where it can interact with the phosphate and carbonyl groups of the lipid, leads to a decrease of the dipole moment, which, however, is less effective than in the case of BAEE because in the case of Arg the carboxylate groups are oriented toward the membrane surface leading to compensate partially the effect due to the guanidyl groups. In turn, as already mentioned, the projection of the carboxylate groups toward the membrane surface leads to a resulting negative zeta potential, as observed experimentally (see Figure 2).

In principle, different types of interactions can be established between phospholipids and Arg or BAEE. For example, the guanidyl and amine (in both Arg and BAEE) and the carboxylic (in Arg) or carbonyl (in BAEE) groups can be expected to establish important interactions with both the membrane and

solvent (all of them can potentially participate in H-bonds). These groups can also be expected to play a major role in stabilizing the crystalline phases of the compounds. Being very sensitive to local changes, in particular felt by polar groups, IR spectroscopy appears as a powerful technique to get some insight on these interactions and, then, provide additional information on the mode of insertion of the two compounds in the membrane.

Figure 4 highlights the $1800-1500$ cm^{-1} region of the FTIR spectra of Arg and BAEE in their dry neat solid state (A, B), 50:50 D_2O solution (C, D), and in DMPC aqueous (D_2O) dispersion (E, F). The bands in this spectral region shall be assigned to the coupled $\delta NH/CN$ in-plane vibrations of the guanidyl moiety, deformational bands of the α-amino group, and stretching modes of carboxylate (in Arg; $-COO^-$) or carbonyl (in BAEE; $-C=O_{Ester/Amide}$) groups.

The spectrum of Arg in the solid state (33% RH) in the considered spectral region shows three main bands (Figure 4A), centered at 1680, 1622, and 1558 cm^{-1}, and a shoulder visible in the higher frequency wing of the 1680 cm^{-1} band. In the same spectral range, the spectrum of neat solid BAEE (Figure 4B) shows a profile similar to that of Arg, with the main bands at 1735, 1652, and 1537 cm^{-1}. According to the calculations, the spectral feature with maximum contribution of the $\delta NH/CN$ mode of the guanidyl moiety in Arg and BAEE should correspond, respectively, to the bands at 1622 and 1652 cm^{-1} (see also Table 2). The relative positions of the bands due to this mode can be expected to serve as sensitive spectroscopic probes of the state of the guanidyl moiety in the different environments studied, the observed frequency shifts being correlated with changes in the strength of the H-bond interactions in which guanidyl moieties are involved or polarity of the local chemical environment.[36,37] The remaining bands observed in the studied spectral region are due to α-amino deformational vibrations and antisymmetric carboxylate (for Arg) or carbonyl (BAEE) stretching vibrations. These latter shall be ascribed to the higher frequency bands in each molecule (bands at 1680 and 1735 cm^{-1}, for Arg and BAEE, respectively).

The IR spectrum of Arg in solution (50:50 D_2O/methanol; Figure 4C) exhibits two main bands: a wide composed band, located at higher frequency (band center at 1642 cm^{-1}), and a well-defined band, at a lower frequency (1560 cm^{-1}). The band's components obtained after deconvolution are located at 1688, 1638, and 1558 cm^{-1}. The corresponding spectrum of BAEE presents three bands (Figure 4D), centered at 1733, 1645, and 1540 cm^{-1}. After deconvolution, the central band appears to be composed of two bands, at 1625 and 1686 cm^{-1}.

It is well-known[38-40] that, except in very special cases, the so-called improper H-bonds,[41] H-bonding leads to a frequency decrease of the stretching vibration of the proton-donor group and simultaneous increase of its bending modes (both in-plane and out-of-plane). A reduction in the stretching frequency upon H-bonding is also expected for a carbonyl (carboxylic ester, BAEE, or acid, Arg) taking part in an H-bond as an acceptor.[37,39] On the other hand, direct comparison of the absolute frequencies (instead of band shifts) is only meaningful if the species which are being compared are closely related structurally because the absolute frequencies are determined not just by force constants but also by the oscillator reduced masses. In the present case, however, comparison of absolute frequencies can be made safely because of the close structural resemblance of Arg and BAEE, in particular, in what concerns their guanidyl fragment.

The differences between the absolute frequencies of the $\delta NH/CN$ mode for Arg and BAEE in aqueous solution are much
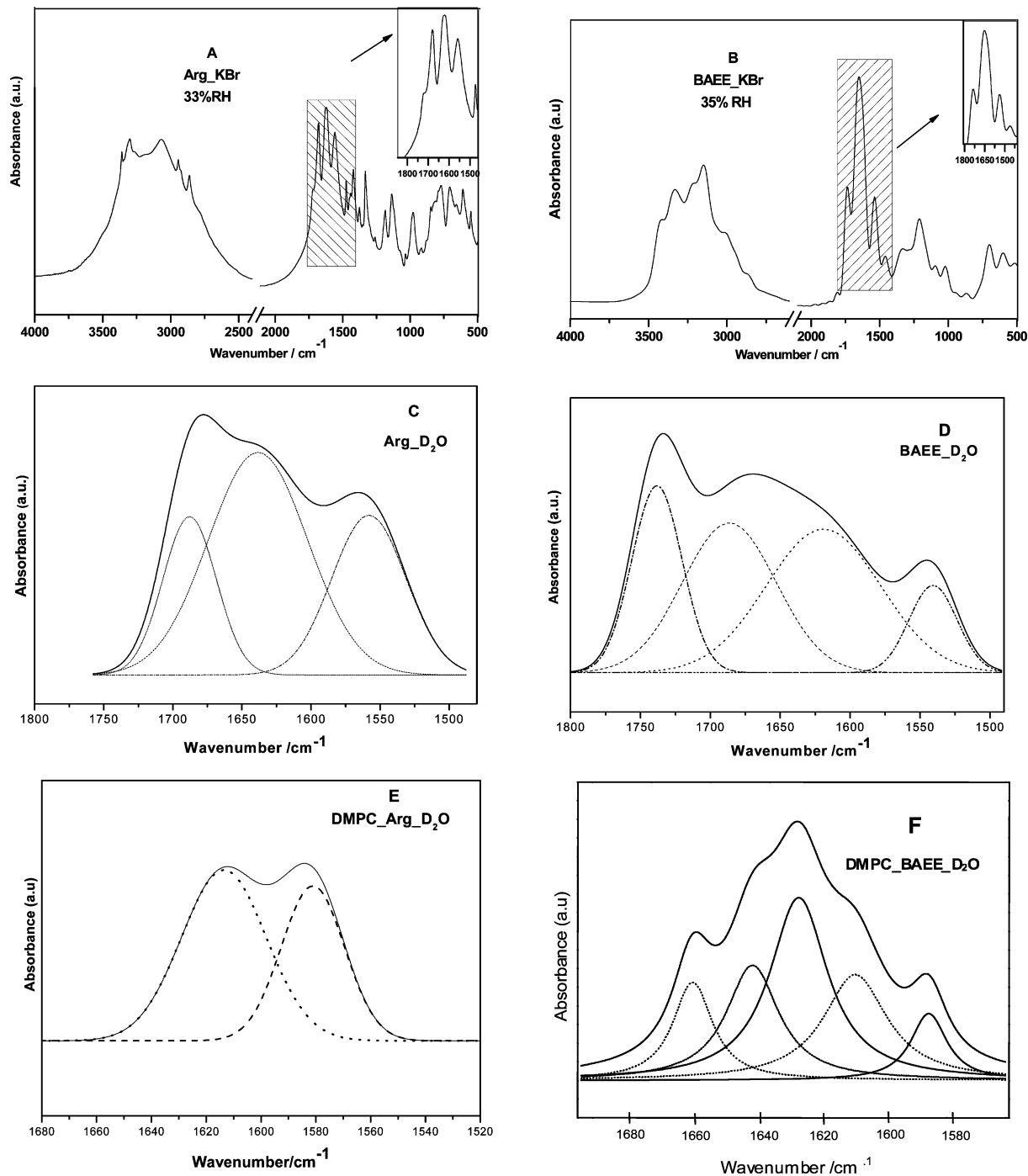
Figure 4. FTIR spectra of Arg and BAEE in: dry solid state (A, B), aqueous solution (C, D), and DMPC aqueous dispersion (E, F). RH: relative humidity.

lower (1638 vs 1625 cm^{-1}) than those between Arg and BAEE in the solid and the aqueous solution (1622 vs 1638 cm^{-1} for Arg and 1652 vs 1625 cm^{-1} for BAEE), indicating that in aqueous solution the guanidyl moiety of the two compounds is in quite similar environments, as expected. Very interestingly, in the dry neat Arg the guanidyl group appears to take part in weaker H-bonds (observed frequency: 1622 cm^{-1}; see Table 2) than those existing in solution (1638 cm^{-1}), whereas the opposite situation seems to occur in BAEE, where the δNH/CN mode gives rise to a higher frequency band (1652 cm^{-1}) than in solution (1625 cm^{-1}).

Let one now look to what happens when Arg and BAEE are transferred to hydrated lipids. The spectrum of Arg dispersed in DMPC lipid in the hydrated state (Figure 4E) shows the band

ascribable to the δNH/CN mode at 1614 cm^{-1}, partially overlapping another band at lower frequency (1580 cm^{-1}). Under the same conditions, BAEE gives rise to a most intense band at 1628 cm^{-1}, corresponding to a component at ca. 1629 cm^{-1} in the deconvoluted spectra (Figure 4F), which is ascribable to the δNH/CN vibration. Thus, it has a direct correspondence with the band at 1614 cm^{-1} observed in the spectrum of Arg dispersed in DMPC lipid in hydrated state (see Table 2).

There are two main conclusions that can be extracted from these results: first, the frequency of the guanidyl δNH/CN vibration decreases for Arg on going from aqueous solution to hydrated DMPC environment; second, this change is nearly absent for BAEE.

TABLE 2: Assignment of the IR Band Due to the δNH/CN Mode of the Guanidyl Moiety of Arg and BAEE in Dry and Hydrated States and Mixed with Dry and Hydrated PC Lipids

	wavenumber/cm^{-1}	
sample	Arg	BAEE
dry solid	1622.0 ± 0.22^a	1652.0 ± 0.28
aqueous solution	1638.3 ± 0.66	1625.0 ± 0.32
mixed with dry lipids	1658.2 ± 0.28	1638.0 ± 0.12
mixed with hydrated lipids	1614.1 ± 0.81	1627.5 ± 0.40

^{a} Uncertainties are standard deviations of at least three different samples (see Materials and Methods section).

The considerably different observed shifts in the guanidyl δNH/CN frequency in Arg on going from aqueous solution to hydrated lipid clearly reveal that the stabilization of Arg in a membrane implies the insertion of the guanidyl moiety of this compound in different environments.

The IR bands due to the vibrations of the guanidyl moiety in BAEE (δNH/CN) show a shift to lower frequencies from dry neat solid (1652 cm^{-1}) to aqueous solution (1625 cm^{-1}) and a subsequent increase from the aqueous solution to the dry lipid environment (1638 cm^{-1}). Thus, when BAEE goes from dry solid to an aqueous solution the strong intermolecular H-bonds that the guanidyl moiety establishes in the crystal are replaced by weaker bonds where the guanidyl moiety acts as a proton-donor and water molecules as proton-acceptors. When BAEE goes from the aqueous solution to the dry lipid environment, the increase in frequency denotes the re-establishment of strong intermolecular H-bonds involving the guanidyl moiety, which are of similar strength of those existing in the crystal.

The negligible variation, within the experimental resolution, of the frequency for BAEE on going from aqueous solution to hydrated lipid (1625 cm^{-1} in aqueous solution and 1628 cm^{-1} in hydrated lipids) clearly reveals that the stabilization of BAEE in a membrane implies the insertion of the guanidyl moiety in a similar environment, i.e., water.

This is in total accordance with the data extracted from zeta potential measurements that indicate that in BAEE the guanidyl groups are essentially exposed to the water phase. On the other hand, in the crystal of Arg the intermolecular H-bonds in which the guanidyl moiety is involved are considerably weaker than those present in the crystal of BAEE since the band due to the δNH/CN vibrations absorbs at much lower frequencies (1622 cm^{-1} for Arg vs 1652 cm^{-1} for BAEE). As was already pointed out, the guanidyl–water H-bonds in aqueous solution are of comparable strength, as expected (the observed frequencies of the δNH/CN band are 1639 cm^{-1} for Arg vs 1625 cm^{-1} for BAEE). Very interestingly, the position of the IR band due to the δNH/CN vibrations of the guanidyl moiety of Arg in dry lipids (1658 cm^{-1}) indicates that the interaction in which this group is involved is even stronger under these conditions than in aqueous solutions. This result is in consonance with the zeta and dipolar potential measurements, which indicate that in the lipid environment the guanidyl moiety of Arg would be facing the phosphate groups, to which they can form strong well-oriented H-bonds. In agreement with this explanation, the frequency of the δNH/CN reduces (1614 cm^{-1}) in going from the dry lipid environment to the hydrated lipid environment, where water molecules located in the nonpolar part of the membrane can compete with the phosphate groups and establish weaker less-specific H-bonds with the guanidyl moiety of Arg. It is also clear from these IR data that the trend shown by Arg to interact with the lipid head groups is particularly relevant since when Arg is mixed with hydrated lipids the band due to the δNH/CN vibrations of the guanidyl moiety appears at the lowest frequency value among all studied systems (1614 cm^{-1}). This indicates that the Arg guanidyl–water interaction in hydrated lipids is much more strongly disturbed by the presence of the lipid head groups than in the case of BAEE under the same conditions (compare the frequency of the δNH/CN band in both cases: 1614 cm^{-1} for Arg vs 1628 cm^{-1} for BAEE).

Conclusions

The DFT(B3LYP)/6-31+G(d,p) calculations indicated that the most stable forms for Arg and BAEE in the presence of water or in strongly polar media (as in the crystalline state) are protonated in the guanidyl moiety, which is in consonance with the experimental data obtained from FTIR and dipole and zeta potential measurements for the compounds in the neat solid state, aqueous solution, and dry and hydrated lipids.

The theoretical calculations also indicated that the most stable cation of BAEE and the most stable zwitterion of Arg should give rise to H-bond sensitive IR bands due to the δNH/CN guanidyl group in the 1700–1500 cm^{-1} range. The relative positions of these bands for BAEE and Arg in the different environments studied could successfully be correlated with the data obtained from both zeta and dipole potential regarding the insertion place and orientation of the two molecules in the lipids. In addition, it also provides some clues regarding the relative strengths of the H-bond interactions involving the guanidyl group in the crystals of the two compounds. Then:

(i) These H-bonds in dry solid Arg are found to be considerably weaker than in BAEE but of comparable strength when the two compounds were dissolved in an aqueous solution; in Arg, the H-bonds in solution are stronger than in the crystal, whereas the opposite occurs for BAEE.

(ii) For BAEE in a lipid environment, the observed decrease in the δNH/CN frequency compared to the neat crystalline state and aqueous solution is consistent with the guanidyl groups of BAEE in the hydrated lipid environment being essentially exposed to the water phase. The reduction of the δNH/CN frequency in going from the aqueous solution to the lipid environment suggests the relevance of geometric constraints imposed by the lipid to the access of water molecules to the guanidyl group of Arg, which is in agreement with the guanidyl group of Arg being placed mainly in the lipid headgroups' region, as deduced from zeta and dipole measurements.

(iii) For Arg in a dry lipid environment, the well-oriented guanidyl–phosphate interactions reflect the establishment of strong H-bonds between these two moieties and consequent increase of the frequency associated with the δNH/CN vibration.

(iv) The picture derived from zeta potentials indicates that the guanidyl moiety of BAEE is exposed to the water phase. Therefore, the dipole moment of BAEE opposes the base dipole potential of the lipid (which is positive inside the membrane), thus explaining the drastic decrease in the dipole potential it induces for both DMPC and DOPC compared to that resulting from the interaction of the lipids with Arg.

Congruently with the IR results, zeta and dipole potential measurements provided direct evidence that Arg orients in a lipid interphase of PC bilayers with the negative carboxylate group ($-$COO$^-$) toward the aqueous phase, whereas the positively charged guanidyl moiety is oriented toward the lipid phase. On the other hand, the guanidyl group in BAEE is oriented in the opposite way, facing the water phase, while the hydrophobic benzoyl and ethyl groups are inserted into the membrane phase.

References and Notes

(1) White, S. H. *J. Gen. Physiol.* **2007**, *129*, 363–369.

(2) De Planque, M.; Kruijtzer, J.; Liskamp, R.; Marsh, D.; Greathouse, D.; Koeppe, R., II; de Kruijff, B.; Killian, J. D. *J. Biol. Chem.* **1999**, *274*, 20839–20846.

(3) Ladokhin, A.; Selsted, M.; White, S. *Biophys. J.* **1997**, *72*, 794–805.

(4) Merino-Montero, S.; Montero, M.; Hernández-Borrell, J. *Biophys. Chem.* **2006**, *119*, 101–105.

(5) MacCallum, J.; Drew Bennett, W.; Tieleman, D. *Exp. J. Gen. Physiol.* **2007**, *129*, 371–377.

(6) Mosior, M.; McLaughlin, S. *Biochemistry* **1992**, *31*, 1767–1773.

(7) Kim, J.; Mosior, M.; Chung, L. A.; Wu, H.; McLaughlin, S. *Biophys. J.* **1991**, *60*, 135–148.

(8) Tung, C. H.; Weissleder, R. *Adv. Drug Delivery Rev.* **2003**, *55*, 281–294.

(9) Zharikov, S.; Block, E. *Biochim. Biophys. Acta, Biomembr.* **1998**, *1369*, 173–183.

(10) Jejoong, Y.; Qiang, C. *Biophys. J.* **2008**, *94*, L61–L63.

(11) Tsogas, I.; Tsiourvas, D.; Paleos, C.; Giastrellis, S.; Nounesis, G. *Chem. Phys. Lipids* **2005**, *134*, 59–68.

(12) MacCallum, J. L.; Bennett, W. F.; Tieleman, P. *Biophys. J.* **2008**, *94*, 3393–3404.

(13) Blokzijl, W.; Engberts, J. B. F. N. *Angew. Chem., Int. Ed. Engl.* **1993**, *32*, 1545–1579.

(14) Iijima, Y.; Hasegawa, S.; Yoshida, M.; Omichi, H.; Yonezawaa, N.; Katakai, R. *J. Chem. Soc., Chem. Commun.* **1993**, *18*, 1399–1400.

(15) MacDonald, R. C.; Simon, S. A. *Proc. Natl. Acad. Sci. U.S.A.* **1987**, *84*, 4089–4093.

(16) Diaz, S.; Lairion, F.; Arroyo, J.; de López, A. C. B.; Disalvo, E. A. *Langmuir* **2001**, *17*, 852–855.

(17) Clarke, R. J. *Adv. Colloid Interface Sci.* **2001**, *89*, 263–281.

(18) Brockman, H. *Curr. Opin. Struct. Biol.* **1999**, *9*, 438–443.

(19) Pohle, W.; Stelle, C.; Fritzsch, H.; Bohl, M. *J. Mol. Struct.* **1997**, *408/409*, 273–277.

(20) Neumann, R.; Nobes, R. H.; Handy, N. C. *Mol. Phys.* **1996**, *87*, 1–36.

(21) Parr, R.; Wang, W. *Density-Functional Theory of Atoms and Molecules*; Oxford University Press: New York, 1994.

(22) Frisch, M. J.; Trucks, G. W.; Schlegel, H. B.; Scuseria, G. E.; Robb, M. A.; Cheeseman, J. R. J.; Montgomery, J. A.; Vreven, T.; Kudin, K. N.; Burant, J. C.; Millam, J. M.; Iyengar, S. S.; Tomasi, J.; Barone, V.; Mennucci, B.; Cossi, M.; Scalmani, G.; Rega, N.; Petersson, G. A.; Nakatsuji, H.; Hada, M.; Ehara, M.; Toyota, K.; Fukuda, R.; Hasegawa, J.; Ishida, M.; Nakajima, T.; Honda, Y.; Kitao, O.; Nakai, H.; Klene, M.; Li, X.; Knox, J. E.; Hratchian, H. P.; Cross, J. B.; Bakken, V.; Adamo, C.; Jaramillo, J.; Gomperts, R.; Stratmann, R. E.; Yazyev, O.; Austin, A. J.; Cammi, R.; Pomelli, C.; Ochterski, J. W.; Ayala, P. Y.; Morokuma, K.; Voth, G. A.; Salvador, P.; Dannenberg, J. J.; Zakrzewski, V. G.; Dapprich, S.; Daniels, A. D.; Strain, M. C.; Farkas, O.; Malick, D. K.; Rabuck, A. D.; Raghavachari, K.; Foresman, J. B.; Ortiz, J. V.; Cui, Q.; Baboul, A. G.; Clifford, S.; Cioslowski, J.; Stefanov, B. B.; Liu, G.; Liashenko, A.; Piskorz, P.; Komaromi, I.; Martin, R. L.; Fox, D. J.; Keith, T.; Al-Laham, M. A.; Peng, C. Y.; Nanayakkara, A.; Challacombe, M.; Gill, P. M. W.; Johnson, B.; Chen, W.; Wong, M. W.; Gonzalez, C.; Pople, J. A. *Gaussian 03*, (Revision D.01); Gaussian, Inc.: Wallingford, CT, 2004.

(23) Becke, A. D. *Phys. Rev. A* **1988**, *38*, 3098–3100.

(24) Becke, A. D. *J. Chem. Phys.* **1993**, *98*, 5648–5652.

(25) Lee, C. T.; Yang, W. T.; Parr, R. G. *Phys. Rev. B* **1988**, *37*, 785–789.

(26) Ditchfield, R.; Hehre, J.; Pople, J. A. *J. Chem. Phys.* **1971**, *54*, 724–729.

(27) Hehre, J.; Ditchfield, R.; Pople, J. A. *J. Chem. Phys.* **1971**, *54*, 724–729.

(28) Scalmani, G.; Barone, V.; Kudin, K. N.; Pomelli, C. S.; Scuseria, G. E.; Frisch, M. J. *Theor. Chem. Acc.* **2004**, *111*, 90–100.

(29) Cossi, M.; Rega, N.; Scalmani, G.; Barone, V. *J. Comput. Chem.* **2003**, *24*, 669–681.

(30) Cossi, M.; Scalmani, G.; Rega, N.; Barone, V. *J. Chem. Phys.* **2002**, *117*, 43–54.

(31) Cossi, M.; Rega, N.; Scalmani, G.; Barone, V. *J. Chem. Phys.* **2001**, *114*, 5691–5701.

(32) Mennucci, B.; Cances, E.; Tomasi, J. *J. Phys. Chem. B* **1997**, *101*, 10506–10517.

(33) Mennucci, B.; Tomasi, J. *J. Chem. Phys.* **1997**, *106*, 5151–5158.

(34) From: [http://www.cem.msu.edu/~reusch/VirtualText/proteins.htm].

(35) Im, J.; Jang, S. W.; Lee, S.; Lee, Y.; Kim, B. *J. Phys. Chem. A* **2008**, *112*, 9767–9770.

(36) Braiman, M. S. *J. Phys. Chem. B* **1999**, *103*, 4744–4750, and references therein.

(37) Sension, R. J.; Hudson, B.; Callis, P. R. *J. Phys. Chem.* **1990**, *94*, 4015–4025.

(38) Jarmelo, S.; Reva, I.; Rozenberg, M.; Ramos Silva, M.; Matos Beja, A. M.; Fausto, R. *J. Phys. Chem. B* **2008**, *112*, 8032–8041.

(39) Jarmelo, S.; Reva, I.; Carey, P. R.; Fausto, R. *Vib. Spectrosc.* **2007**, *43*, 395–404.

(40) Jarmelo, S.; Reva, I.; Rozenberg, M.; Carey, P. R.; Fausto, R. *Vib. Spectrosc.* **2006**, *41*, 73–82.

(41) Govender, M. G.; Ford, T. A. *J. Mol. Struct. THEOCHEM* **2003**, *630*, 11–16.